J Solid State Electrochem (2003) 7: 223–231
DOI 10.1007/s10008-002-0307-2

ORIGINAL PAPER

Moein B. Sayed

Solid state a.c. conductivity and FT-IR spectral analyses for the conflicting effects of proton mobility and association in some azophenol derivatives of cyclic phosphazene

Received: 21 January 2002 / Accepted: 5 July 2002 / Published online: 30 August 2002

Abstract Variable strength H-bonding affects the mobility and so electric conduction of protons differently. Also, variable extent mesomerism modifies electric conduction with varying dielectric features. Both these molecular modifiers are properly cited using azophenol derivatives as model compounds for discussion of their consequences in the varying features of electric conduction. The electric permittivity shows low-frequency dispersion characteristic of ionic conduction over mobile charge carries; the mobility shifts at a critical temperature T_c, being structure dependent. The frequency-dependent Z''-Z' layout changes with temperature from linear at low temperatures to semicircular above T_c within a frame of temperature-sensitive dipole-ionic mediated conduction. The a.c. conductivity, σ_{ac}, increases with frequency and temperature and becomes frequency insensitive, like d.c. conductivity, σ_{dc}, above the T_c because of the escalating contribution from the d.c. conduction. The mesomeric structure seems to prompt a dipole-based electric conduction of high relaxation energy over the strongly associated phenolic protons that may be thermally activated above the T_c into a much lower relaxation energy protonic conduction of up to two orders higher conductivity. The protonic conduction emerges at a T_c that falls with a drop in the relaxation energy following a similar order of increasing proton mobility and mesomerism in the azophenol derivatives: azocatechol > azoquinol > azoresorcinol. On the molecular level, variable temperature infrared spectroscopy reveals higher proton mobility and mesomerism for the azocatechol derivative that demonstrates its higher protonic conductivity at lower T_c and relaxation energy, compared to the azoquinol and azoresorcinol derivatives. This is well verified in the light of conflicting intramolecular H-bonding that assists the proton mobility in azocatechol whereas it associates the protons in azoresorcinol more than in azoquinol.

M.B. Sayed
Chemistry Department,
Al-Azhar University, Cairo, Egypt
E-mail: mbsayed@hotmail.com

Introduction

Cyclic phosphazenes are of interest as they afford mesomerism sufficient for activating the atoms attached to the phosphazene ring. The hexachloro derivative of cyclotriphosphazatriene, HCCTP, undergoes reactions to yield geminally bis [1], tetrakis [2] and fully [3] substituted derivatives. Similarly, synthesis of the fully substituted azo derivatives (Scheme 1) of phenol, catechol, resorcinol and quinol has been successfully performed [4, 5] from the hexaamido derivative. Despite the symmetric coupling, the three pairs of geminally substituted azo linkages orient differently because of ring puckering known to distort the CTP structure in the solid state [5, 6, 7]. The azo derivatives showed inter- and intramolecular H-bonding of different thermodynamics [5]. Intramolecular H-bonding mobilizes the catechol proton *para* to the azo linkage (Scheme 2A), whereas it associates the phenolic proton *ortho* to the azo linkage (Scheme 2B) in a stable six-membered ring for the azoresorcinol more than the azoquinol derivative. At variance, intermolecular H-bonding influences the structure with a lesser discriminating role. Such different H-bonding associations are identified on the molecular level using variable temperature FT-IR spectroscopy.

In the diazotization of hexaamidocyclotriphosphazatriene, HACTP, the fully protonated HCl salt could be isolated in a pure state and showed unusual capacitance and fast ion features [6]. Extending the molecular mesomerism and associating the conducting ions modify the unusual high conductivity features into a dipole-protonic mediated conduction of much lower conductivity in the more mesomeric but less ionic hexaazophenol derivative [7].

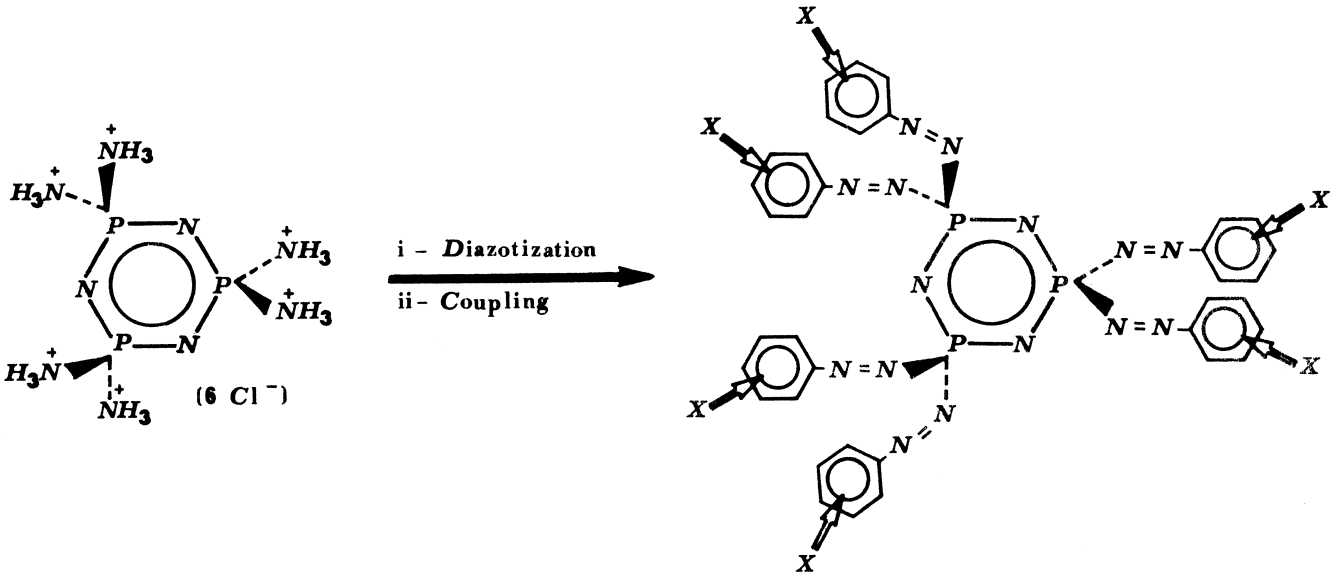

Scheme 1 Diazotization and coupling of HACTP-HCl with phenols (X = catechol, quinol or resorcinol)

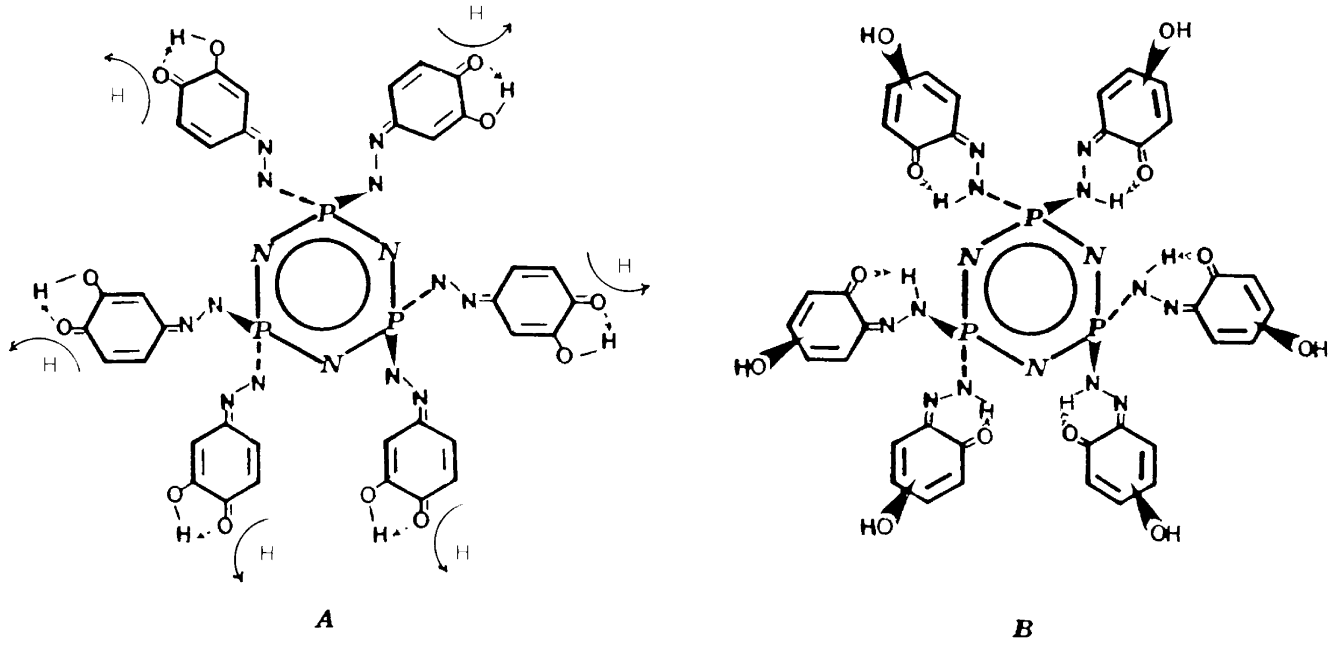

Scheme 2 **A** Proton mobility-assisted mesomerism in the azocatechol derivative. **B** Associated protons retard mesomerism in the azoresorcinol more than the azoquinol derivative

The aim of the present work is to extend analysis on the molecular level [6, 7] by a.c. conductivity and FT-IR spectroscopy to the role of variable H-bonding and mesomerism [4, 5] that is supposed to influence the electric features in the azophenol derivatives to different extents. This could be well illustrated by systematically varying the measurement temperature and reading the variation in the electric and spectral features at intervals throughout the range.

Experimental

Materials

The azophenol derivatives were prepared by diazotization of HACTP-HCl (Scheme 1) and coupling of its multifunctional diazonium salt with the phenols [8]. The coupling was immediate. However, the azo derivatives required prolonged periods of time [4, 5] for reaction to lead to a full symmetric substitution and for extraction to yield pure shiny dark brown crystals from pure

ethanol. Full substitution is evident by the absence of NH_2 and replacement by the -N=N- feature. The compounds were thermally characterized by DTA [5] and by variable temperature FT-IR spectroscopy [9, 10]. DTA showed decomposition of the azo linkages in three distinct stages [5]; their thermodynamics varied with the variation in the H-bonding association and mesomerism in the azophenol derivatives. The thermal data showed higher ΔC_p, ΔH and ΔS but lower $E^{\#}$ values for the decomposition stages for the azocatechol than for the azoquinol than for the azoresorcinol derivatives. Such DTA data illustrate the conflicting effects of proton mobility and association on the molecular structure of the present azophenol derivatives. The mobile catechol protons weakened the N=N into more disordered N-N linkages (Scheme 2A) so that they decomposed at lower activation energies but with higher enthalpy and entropy changes. In contrast, the azo linkages are protected by intramolecular H-bonding association (Scheme 2B) so that they decompose at higher activation energies with lower enthalpy and entropy changes in azoresorcinol than azoquinol, compared to the azocatechol having no protons *ortho* to the azo linkage.

Methods and equipment

Infrared spectra of the azo derivatives were measured at varying temperatures, using KBr discs, a Graseby Specac variable-temperature cell (293–623 K) and a Nicolet 510P FT-IR spectrometer. Dependence of the electric impedance, Z, capacitance, C, and phase angle, $n\pi/2$, on the frequency (0.6–600 kHz) and temperature (373–623 K) was measured for the azophenol derivatives in the solid state far below the decomposition temperature [5] at 0.8 V, using a Hioki LCR 3520 Hi-tester. The electric measurements below 373 K were excluded because of the perturbing effect of sorbed water that acts as a vehicle assisting the proton mobility and therefore protonic conduction [11, 12]. Desorption lowers the electric conductivity to a minimum (or raises its impedance to a maximum) at 373 K, the boiling temperature of water. This has been shown to occur before the conductivity rises with temperature on gaining the activation energy required for promoting the protonic conduction. The electric measurements were performed for 0.1-cm thick 1 cm^2 discs that were firmly held at the sample/electrode interface. The electric data were treated as prescribed elsewhere [6, 7, 11, 12, 13, 14, 15].

Results and discussion

Analysis and discussion of the data are referred to the azocatechol derivative; correlation with the other azo derivatives is made wherever useful. The impedance Z separates into real Z' and imaginary Z'' parts set apart by the phase angle $\cos n\pi/2$ and $\sin n\pi/2$ derivatives, with $j=(-1)^{1/2}$:

$$Z = Z' - jZ'' = Z\cos n\pi/2 - jZ\sin n\pi/2 \quad (1)$$

In ionic compounds, the Z''-Z' dependence is distinguished by a Cole-Cole semicircular diagram [6], characteristic of ionic relaxation [11, 12, 13, 14, 15, 16, 17, 18, 19, 20, 21, 22, 23] for an RC circuit in which the bulk capacitance is in parallel with the bulk resistance and

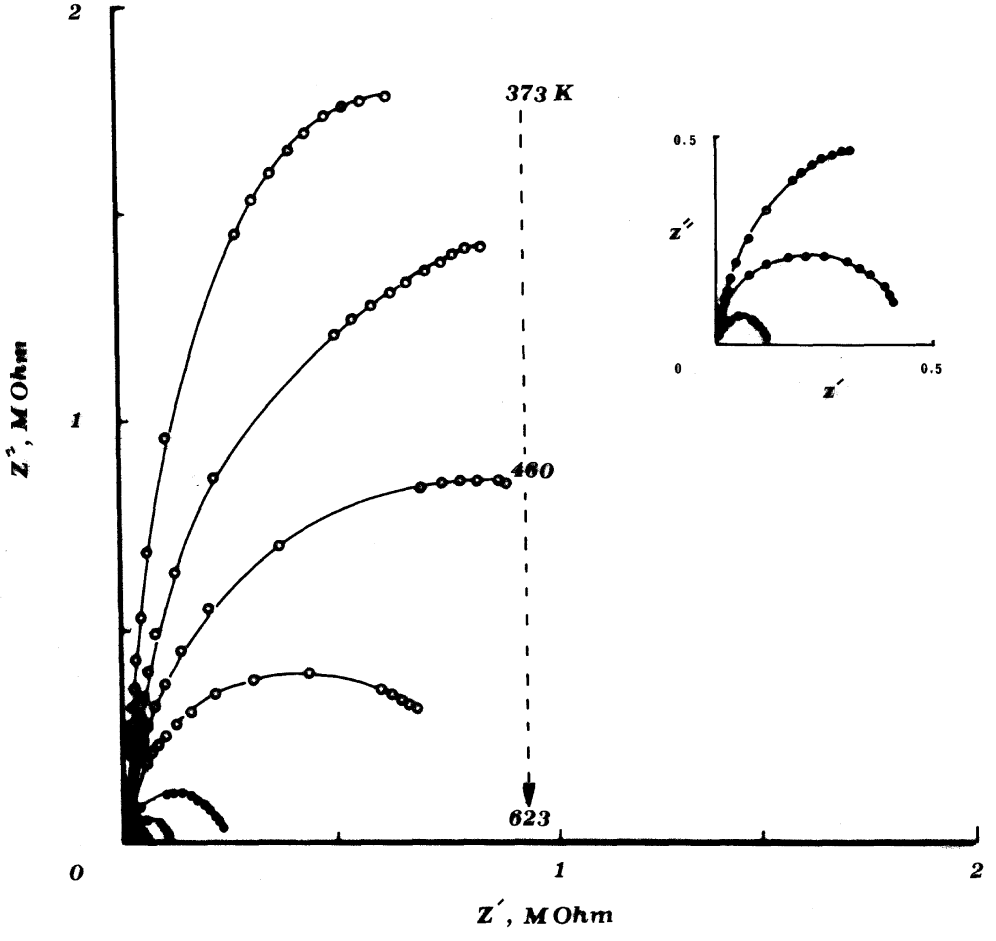

Fig. 1 Variable frequency Z''-Z' dependence of azocatechol at 373, 428, 460, 498, 548, 583 and 623 K. The *inset* correlates this dependence for (*bottom to top*) azocatechol, azoquinol and azoresorcinol at 583 K

is in series with another sample/electrode interfacial capacitance:

$$Z' = R/1 + (\omega RC)^2; \quad Z'' = \omega R^2 C/1 + (\omega RC)^2 \qquad (2)$$

In such ionic conduction, the d.c. resistance R_{dc} may indirectly be driven by extrapolating the Z''-Z' dependence to the d.c. frequency, ω_{dc}. Z' reads as R_{dc} when Z'' vanishes at the zero ω_{dc} frequency. This facilitates an indirect method for estimating the d.c. conductivity, σ_{dc}, as will be shown later. The Z''-Z' dependence turns to linear upon increasing the perturbation of the well-oriented ionic conduction with scattered dipole interactions that dominate at relatively low temperatures [7, 14, 15]. The Z''-Z' layout of this work (Fig. 1) alternates between linear and semicircular dependencies separated by a critical temperature T_c at which the conduction changes mechanism. At low temperatures, the Z''-Z' dependence is dominantly linear, suggesting a dipole-based electric conduction over the strongly associated phenolic protons [7]. At 488 K the protons gain a thermal energy sufficient for promoting a protonic conduction, which is recognized by the Cole-Cole semicircular dependence. Correlating the impedance dependence at 583 K (Fig. 1, inset) reveals a higher tendency to protonic conduction for the azocatechol more than for the azoquinol and much more than for the azoresorcinol derivatives.

The electric impedance Z' and Z'' may also be illustrated independently as they change with frequency ω and temperature T. Z' (Fig. 2) and Z'' (Fig. 3) are less dependent on ω below 10 kHz. The frequency-least dependent on Z_0' (measured arbitrary at 0.6 kHz) rises with T to a maximum at 488 K (Fig. 2, inset), owing to a drop in the dipole interaction as a result of the thermal scattering effect. The subsequent drop in Z_0' at higher temperatures corresponds with the appearance of electric features characteristic of protonic conduction. For instance, Z'' shows a protonic relaxation loss band (Fig. 3) shifting exponentially with temperature (Fig. 3, inset, Eq. 3) to higher frequencies [23]. The average relaxation energy of this protonic conduction, E_{Rel}, as calculated from the slope of the logarithmic dependence of Eq. 3, is 0.55 eV, and the time τ calculated from the intercept is 8.55×10^{-10} s:

$$\omega_{max} = \omega_0 \exp(-E_{Rel}/kT) \qquad (3)$$

where ω_0 is the angular frequency at ∞T, k is Boltzmann's constant and E_{Rel} is the average ionic relaxation energy.

E_{Rel} and τ are correlated for the azophenol derivatives in Table 1. The protonic conduction in azocatechol is activated at lower E_{Rel} (0.55 eV) and T_c (488 °K) than for azoquinol (0.89 eV and 513 °K). The phenolic

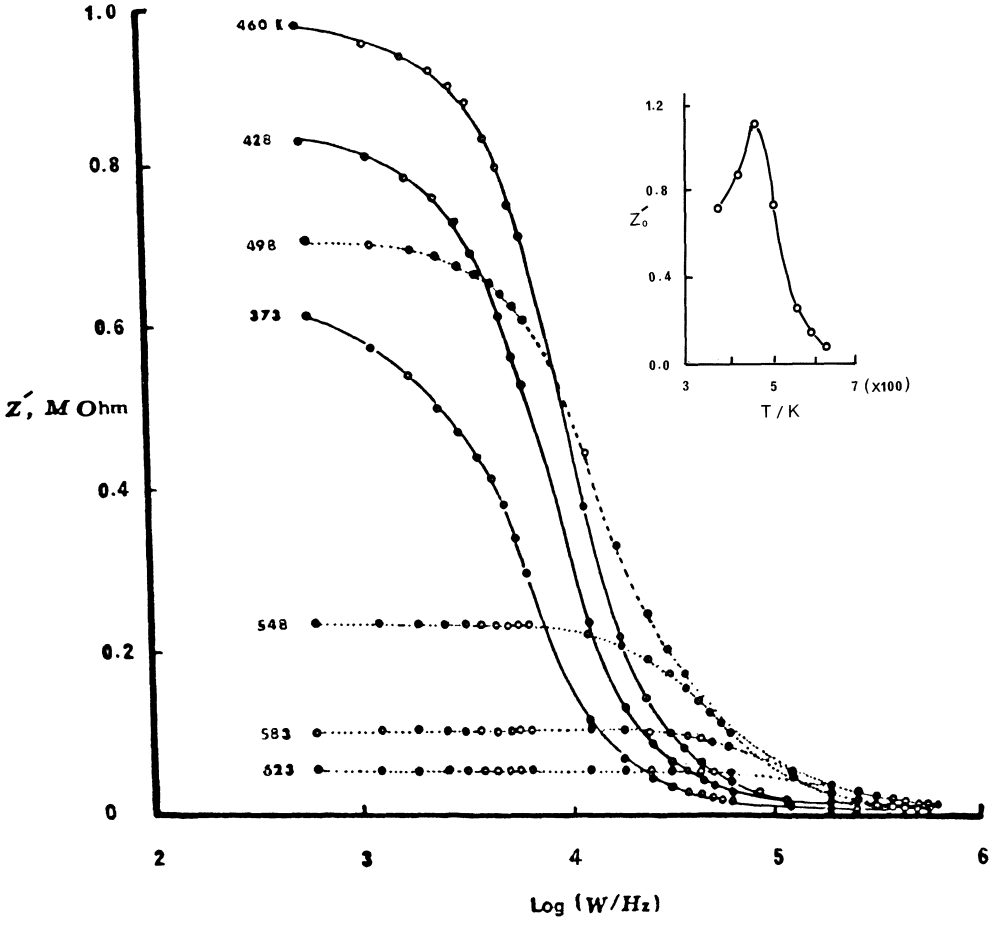

Fig. 2 Change in Z' with ω at 373, 428, 460, 498, 548, 583 and 623 K for azocatechol. The *inset* shows the change in the frequency least dependent Z_0' (measured at 0.6 kHz) with T

protons in the azoresorcinol derivative are so firmly associated that its dipole-based electric conduction has insignificantly changed even at the correlation temperature of 583 K.

Discussion of the variation in the protonic conduction may be furnished at the molecular level, based on the varying extents of H-bonding association and molecular mesomerism. This is supported by a solid state FT-IR spectral analysis over a similar range of temperatures. Spectral correlation shows a high extent of H-bonding in azoresorcinol (Fig. 4e, f), but a low amount in azocatechol (Fig. 4a, b). Intramolecular H-bonding mobilizes the azocatechol proton *para* to the azo linkage (Scheme 2A) that assists protonic conduction, while it associates the azoresorcinol proton *ortho* to the azo linkage in a stable six-membered ring (Scheme 2B) that makes transfer to the protonic conduction difficult. The remote phenolic proton of the latter solid is also associated via intermolecular H-bonding. Spectral subtraction at 583 K shows similar results for azoquinol and azoresorcinol (Fig. 5c–d and Fig. 5e–f), on the one hand, and for azocatechol and azophenol (Fig. 5a–b and Fig. 5, bottom) on the other hand. However, they commonly show three $\nu_{O\text{-}H}$ bands (Fig. 5) in the vicinity of 3000 cm^{-1} that agree with the puckered CTP ring distinguishing orientation of the attached three phenolic pairs [6, 24]. Persistence of these bands upon heating of the azoresorcinol derivative at the correlation temperature of 583 K (Fig. 4e, f) precludes any significant role of proton mobility in its electric conduction. In contrast, these three bands merge (Fig. 4a, b) at the lower frequency $\nu_{O\text{-}H}$ band for azocatechol; the lower frequency band is associated with the phenolic proton of higher acidity, i.e. mobility. At variance, they merge at the mid-frequency band (Fig. 4c, d) associated with the phenolic proton of mid-acidity in azoquinol. Conduction is then greatly assisted by the greater phenolic proton mobility in azocatechol than in azoquinol, compared to the persistently associated azoresorcinol. Merging the three $\nu_{O\text{-}H}$ absorptions into one indicates removal of the CTP ring puckering that affords a better orientation for the attached phenolic groups, which in turns assists the protonic conduction over the terminal phenolic protons. Similar to the impedance correlation at 583 K, further spectral analysis is performed at the same temperature and reveals the following data.

The $\nu_{C=O}$ mode appears in the range 1707 ± 7 cm^{-1} [azocatechol (1700 cm^{-1}) < azoquinol (1707 cm^{-1}) < azoresorcinol (1714 cm^{-1})]. The phenyl ν_{ring} breathing appears in the range 1610 ± 7 cm^{-1} [azocatechol (1603 cm^{-1}) < azoquinol (1611 cm^{-1}) < azoresorcinol (1617 cm^{-1})]. The $\nu_{N=N}$ mode appears in the range

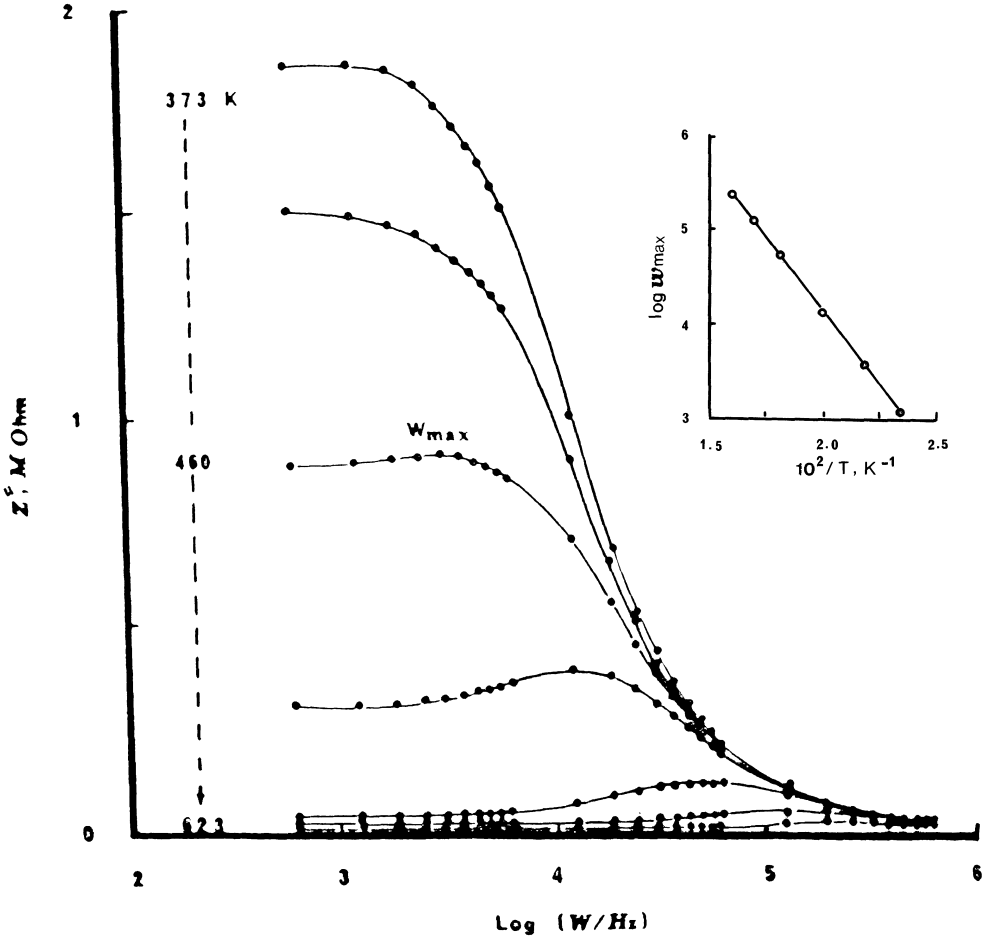

Fig. 3 Change in Z'' with ω at 373, 428, 460, 498, 548, 583 and 623 °K for azocatechol. The *inset* shows exponential rise in the relaxation loss band frequency (or linear rise in log ω) with T

Table 1 Correlation of the electric features for the azo CTP derivatives

Derivative	T_c (K)	d.c. conductivity[a]			a.c. conductivity[a]			E_{Rel} (eV)	τ (s)
		E_d (eV)	E_p (eV)	σ_{dc} ($\times 10^{-7}$) (ohm^{-1} cm^{-1})	E_d (eV)	E_p (eV)	σ_{ac} ($\times 10^{-7}$) (ohm^{-1} cm^{-1})		
Azocatechol	488	0.10	0.72	0.27–13.00	0.20	0.56	0.02–01.07	0.55	8.6×10^{-10}
Azoquinol	513	0.05	0.72	0.19–03.00	0.12	0.56	0.02–00.35	0.89	1.0×10^{-11}
Azoresorcinol	518	0.05	0.12	0.18–00.41	0.12	0.40	0.01–00.08	Almost absent	

[a] σ_{ac} (measured at 125 kHz) and σ_{dc} are correlated in the temperature range 373–623 K. E_d and E_p are the activation energies for the dipole-protonic mediated electric conduction

1400 ± 2 cm^{-1} [azocatechol (1398 cm^{-1}) < azoquinol (1400 cm^{-1}) < azoresorcinol (1402 cm^{-1})]. The CTP ν_{ring} breathing appears in the range 1222 ± 22 cm^{-1} [azocatechol (1200 cm^{-1}) < azoquinol (1229 cm^{-1}) < azoresorcinol (1244 cm^{-1})].

The larger spectral shift of ± 22 cm^{-1} observed in the CTP ν_{ring} mode assigned at 1222 cm^{-1} demonstrates higher sensitivity to changes in the molecular mesomerism [9]. Azocatechol affords higher proton mobility and mesomerism explicit in lower bond orders, shown in lower vibrational wavenumbers that makes the correlation data of Table 1 comprehensive and more conclusive.

As for the electric impedance, the permittivity ϵ combines real ϵ' and imaginary ϵ''components; they

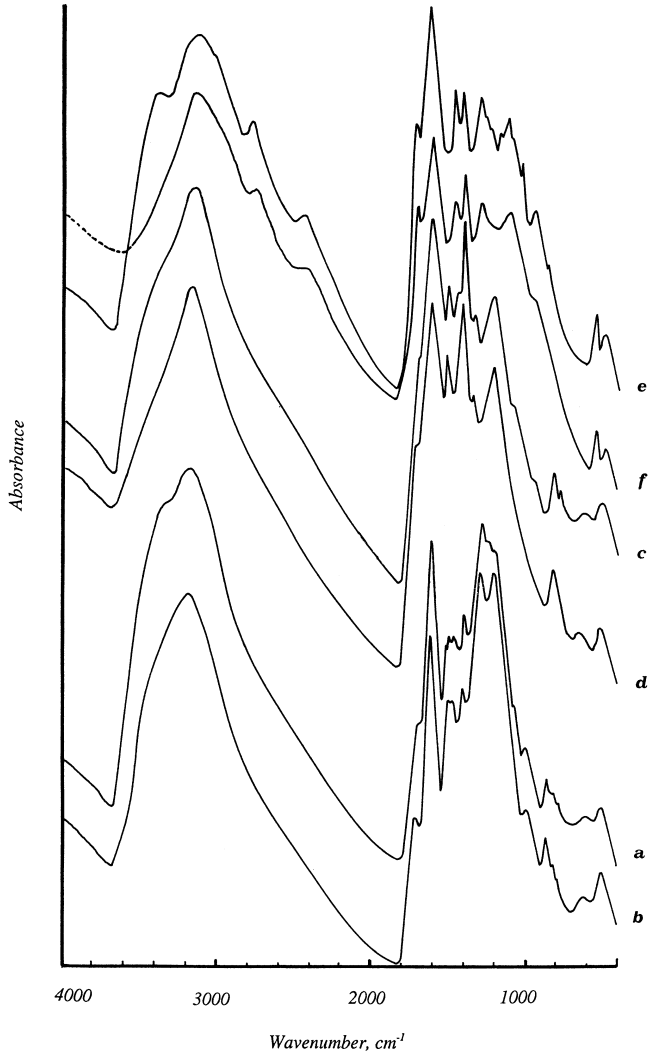

Fig. 4 IR spectrum of azocatechol (*a*, *b*), azoquinol (*c*, *d*) and azoresorcinol (*e*, *f*) in the range 293–583 K

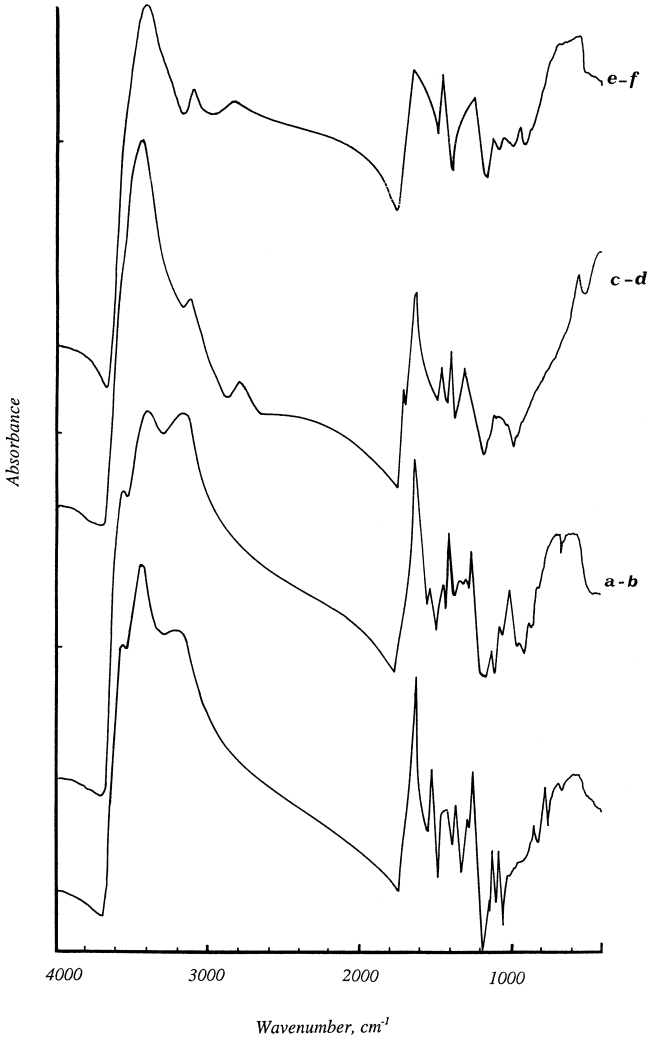

Fig. 5 Spectral subtraction (583–293 K) for (*a–b*) azocatechol, (*c–d*) azoquinol and (*e–f*) azoresorcinol, compared with azophenol at the *bottom*

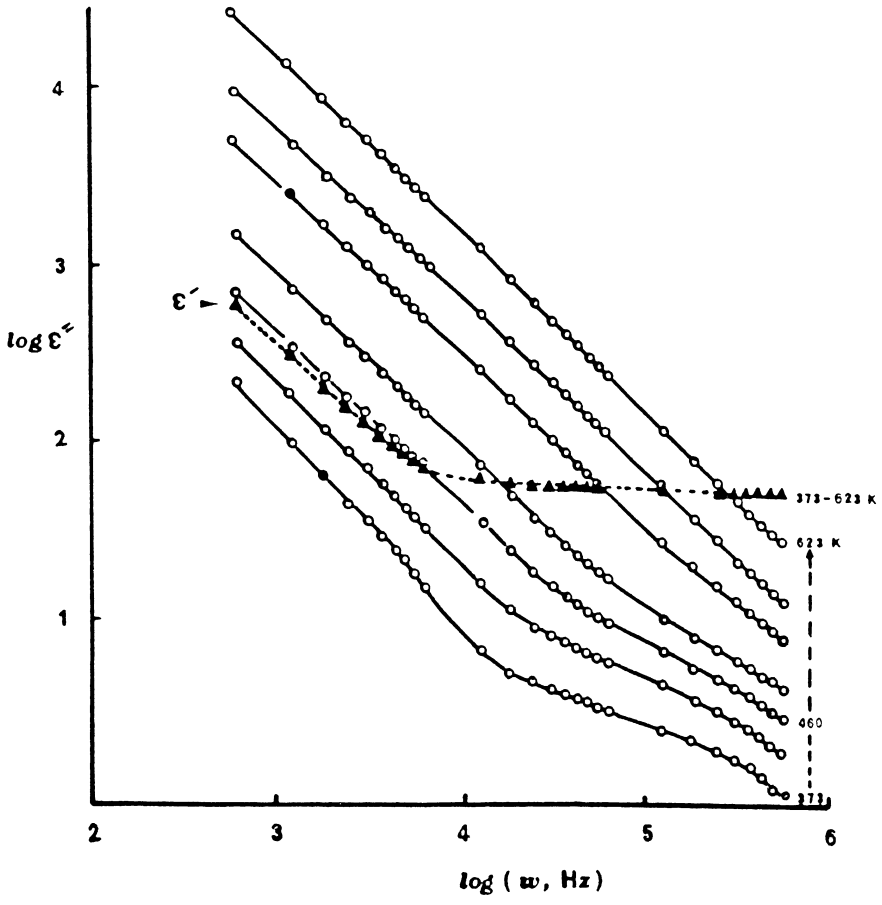

Fig. 6 Logarithmic dependence of the permittivity components ϵ' and $\epsilon''$of azocatechol on ω at 373, 428, 460, 498, 548, 583 and 623 K. ϵ' increases but only very slightly with temperature

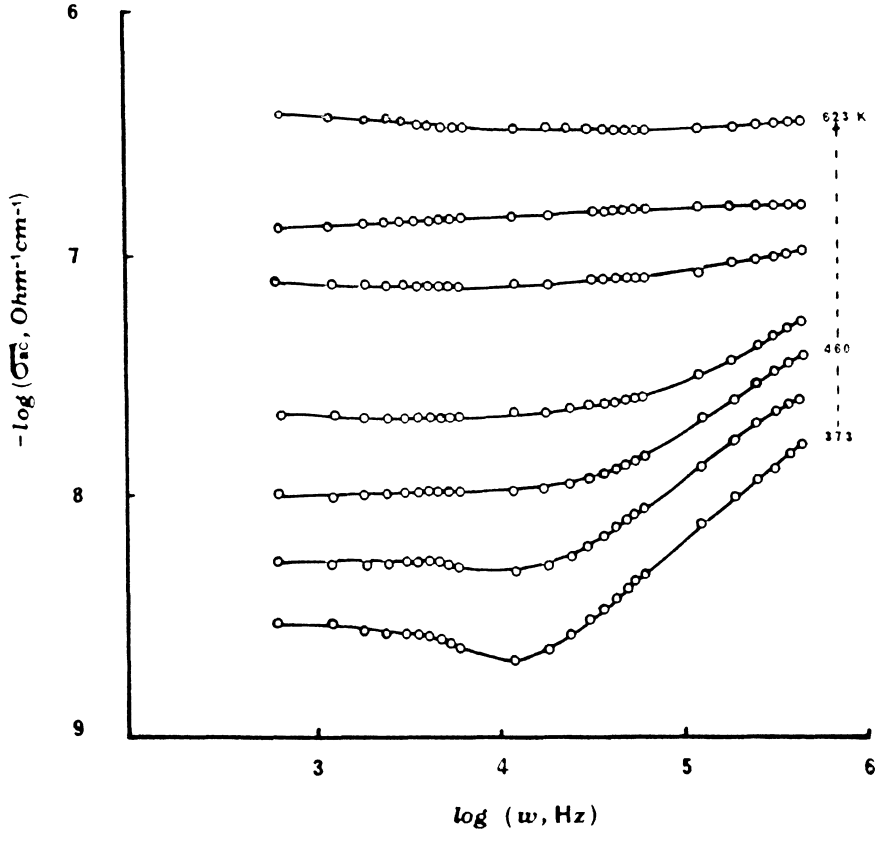

Fig. 7 Logarithmic dependence of the a.c. conductivity σ_{ac} on ω for azocatechol at 373, 428, 460, 498, 548, 583 and 623 K

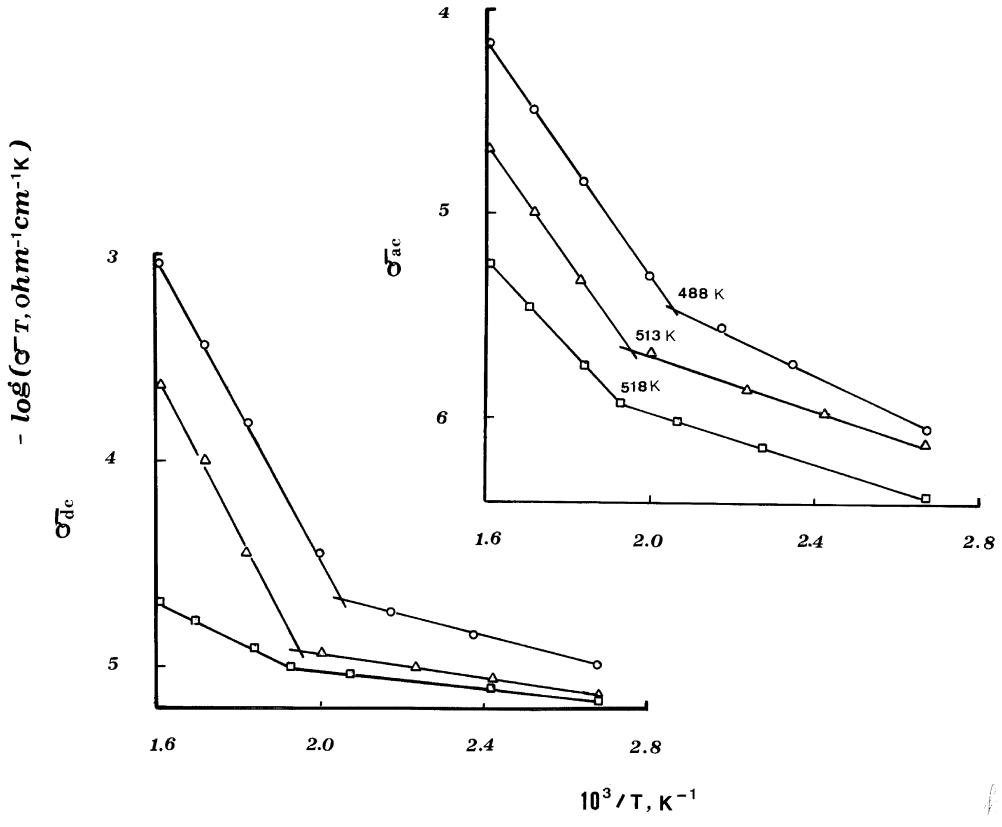

Fig. 8 Arrhenius dependence of σ_{ac} and σ_{dc} on T for azocatechol (*circles*), azoquinol (*triangles*) and azoresorcinol (*squares*)

essentially measure the dielectric constant and loss within the target samples, respectively. They depend on frequency ω (Fig. 6) following the universal fractional power law [25, 26, 27, 28, 29] of Eq. 4:

$$\varepsilon \propto \omega^{S-1} \tag{4}$$

They show low-frequency dispersion (LFD) indicative of conduction via mobile charge carriers that impart polarization, leading to d.c. conduction at elevated temperatures [30, 31]. ϵ' retains the LFD throughout the temperature range; ϵ'' changes dependence on ω significantly above the T_c. Above 10 kHz, the slope of the ω-dependent ϵ'' increases with T (Fig. 6) owing to a progressive drop in the exponent S to eventually zero, where it merges with the higher value slope below 10 kHz. This demonstrates the role of the increasing contribution from d.c. conduction at high temperatures. The relaxation energy E_{Rel} falls with the drop in the exponent S (Eq. 5) on raising the measurement temperature, tending to the more dominant protonic conduction at elevated temperatures [7, 32]:

$$1 - S = (6k/E_{Rel})T \tag{5}$$

Considering the disc thickness d and area A or the cell constant d/A, the d.c. σ_{dc} and a.c. σ_{ac} kinds of electric conductivity are assessed on the electric impedance and permittivity, respectively. σ_{dc} is calculated from the d.c. resistance R_{dc} (Eq. 6), which in turn is measured as the value of Z' when Z'' tends to zero upon extrapolating the Z''-Z' semicircles of Fig. 1 to zero ω_{dc} frequency:

$$\sigma_{dc} = (d/A)(1/R_{dc}) \tag{6}$$

σ_{ac} is calculated from the dielectric loss ϵ'' (Eq. 7), which in turn is measured as $\epsilon' \tan n\pi/2$, with ϵ' being C'/C_0 and C_0 is $[A/d]\epsilon_0$, where ϵ_0 is the vacuum permittivity [6, 7, 11, 12, 13, 14, 15, 16, 17]:

$$\sigma_{ac} = \omega\varepsilon'' \tag{7}$$

σ_{ac} for ionic materials is supposed to rise with frequency (Eq. 7) and temperature (Eq. 8). The latter thermal parameter is known to enhance the ion mobility μ and population of the mobile ions n:

$$\sigma = ne\mu \tag{8}$$

n depends on the temperature as $n = n_0 e^{S_f/K} e^{-E_f/KT}$, where S_f and E_f are the entropy and enthalpy of ion formation.

The temperature dependence of the ion mobility is $\mu = \mu_0 e^{-E_m/KT}$, where E_m is the ionic activation energy. This is shown at low temperatures far away of the contribution from the d.c. conduction (Fig. 7) over 10 kHz.

Like σ_{dc}, σ_{ac} levels into a plateau value above T_c because of the rising contribution from the polarization-induced d.c. conduction. In effect, σ_{dc} leads σ_{ac} by one order (Table 1) of higher magnitude. Since the polarization-induced extraordinary high d.c. conduction is

more prominent above T_c, where the protonic conduction is prominent, a possible source might be transfer of the azo compounds into an unusual phase like that found for liquid crystals. Evidence for this is that the merging of the three $\nu_{O\text{-}H}$ into one should not occur unless distortion due to ring puckering is removed, which would not happen without ultimate transfer of the solid material into a phase of higher mobility.

Based on the Arrhenius dependence (Eq. 9) of $\log \sigma T$ on T^{-1}:

$$\log \sigma T = \log A - (E^{\#}/R)T^{-1} \quad (9)$$

the plots above T_c (Fig. 8), where the conduction is dominantly protonic, show the conductivity rising to higher magnitudes at reduced T_c (Table 1) in the azo derivatives following the order: azocatechol > azoquinol > azoresorcinol.

About two times higher activation energy is required to promote the dipole-based electric conduction in the azocatechol derivative to the protonic mechanism at much lower protonic relaxation energy and lower T_c of 488 K (Table 1), compared to the azoquinol derivative at 513 K. This leads to a protonic conduction of two orders higher conductivity in azocatechol, compared to only one order higher conductivity in azoquinol. The low dipole-based electric conduction has rather insignificantly shifted in the strongly associated azoresorcinol derivative.

Conclusions

On the molecular level, the present study details the sensitive dependence of electrical features on the molecular status of proton mobility and mesomerism in azophenol derivatives. The azocatechol derivative shows high proton mobility and mesomerism (Scheme 2A) that assist the protonic conduction at low T_c and relaxation energy. In contrast, the azoresorcinol derivative shows much lower proton mobility and mesomerism (Scheme 2B) under the impact of reinforcing inter- and intramolecular H-bonding association that stands against similar promotion of the dipole-based conduction into the protonic mechanism. Azoquinol, on other hand, is distinguished by rather moderate figures of such contrasting effects of the molecular and conductivity features. Variation in the conflicting impacts of proton mobility and association is well recognized for the azophenol derivatives on the electrical features throughout their stability range (this work) as well as on the thermodynamics [5] of their azo linkage decomposition.

References

1. Finncham JK, Hurstshouse MB, Parkes HG, Shaw RA (1986) Acta Crystallogr Sect B 42:462
2. Shaw RA (1976) Z Naturforsch B 31:641
3. Das SK, Keat R, Shaw RA, Smith BC (1965) J Chem Soc 5032
4. Sayed MB, Kassem ME, Ibrahim EHM, Al-Emadi IM (1992) Thermochim Acta 197:161
5. Sayed MB, Ibrahim EHM, Al-Emadi IM (1992) Thermochim Acta 198:21
6. Sayed MB (2000) Solid State Ionics 128:191
7. Sayed MB (2001) Solid State Ionics 138:305
8. Blangey FD (1949) Fundamental processes of dye chemistry. Interscience, New York
9. Thomas LC (1974) Interpretation of the infrared spectra of organophosphorus compounds. Heyden, London
10. Bellamy LJ (1975) The infrared spectra of complex molecules. Chapman and Hall, London
11. Sayed MB (2000) Micro- and Meso-porous Mater 27:107
12. Sayed MB (1992) J Phys Chem Solids 53:549
13. Sayed MB (1992) J Phys Chem Solids 53:1041
14. Sayed MB (1996) Microporous Mater 6:181
15. Sayed MB (1996) Qatar Univ Sci J 16:61
16. Powles JG (1953) J Chem Phys 21:633
17. Al-Allak HM, Brikman AW, Russel GJ, Roberts AW, Woods J (1988) J Phys D Appl Phys 21:1226
18. Alexandrova IP, Moskovich YuN, Rozanov OV, Sukhovsky AA (1984) Ferroelect Lett 1:131
19. Baranov AI, Fedosyuk RM, Schogina NN, Shuvalov LA (1984) Ferroelect Lett 2:25
20. Pawlaczyk Sz, Salman FE, Pawlawoski A, Szapela Z, Pietraszko A (1986) Phase Transitions 8:9
21. Kanno R, Takeda Y, Takada K, Yamamoto O (1984) J Electrochem Soc 131:469
22. Takeda Y, Kanno R, Kawatsu S, Yamamoto O (1986) J Mater Sci Lett 5:73
23. Hilczer B, Pawlaczyk C, Salman FE (1988) Ferroelectrics 81:193
24. Manfait M, Alix AJP, Labarre JF, Sourries F (1982) J Raman Spectrosc 12:212
25. Jonscher AK (1983) Dielectric relaxation in solids. Chelsea Dielectrics, London
26. Niklasson GA (1987) J Appl Phys 62:R1
27. Jonscher AK (1990) Electrochim Acta 35:1595
28. Jonscher AK (1991) Universal relaxation law. Chelsea Dielectrics, London
29. Dyre JC, Schroder TB (2000) Rev Mod Phys 72:3
30. Dissado A, Hill RM (1984) J Chem Soc Faraday Trans 2 80:291
31. Bates JB, Wang JC (1988) Solid State Ionics 115:28
32. Mansingh A, Dhar A (1985) J Phys D Appl Phys 18:2059